Automated Perching of a Multirotor UAV atop Round Timber Posts

Tzu-Jui Lin, Siyu Long, and Karl A. Stol, *Member, IEEE*

***Abstract*— Multirotor UAVs currently suffer from endurance issues due to limited battery capacity, greatly limiting their use for surveillance tasks in fields such as agriculture. To remedy this, we have developed a system used for perching of multirotor UAVs onto farm posts. The paper consists of two major sections: design and testing of a perching mechanism and design and testing of a computer vision based system for automated landing. Static experiments and flight testing of the completed system suggests that the design can withstand wind forces once perched and landing success is directly linked to the landing accuracy of the craft. However, performance of the controller was unsatisfactory during tests with wind, where further work could be completed.**

I. Introduction

Recent advancements in technology has granted access to low-cost, high performance inertial measurement units and microprocessors, leading to a new family of unmanned aerial vehicles (UAVs) known as multi-rotor UAVs. In contrast to more traditional fixed-wing UAVs, multi-rotor UAVs offer advantages such as the ability to hover at a fixed location and possession of high agility, allowing for complex flight maneuvers. Coupled with low costs of hardware, multi-rotor UAVs have found extensive uses in industries such as power with surveying of power lines [1] and agriculture, surveying crop health. [2] However, high energy consumption and lackluster battery technologies heavily restrict the flight time of multi-rotor UAVs, limiting their use for perch-and-stare missions. Perch-and-stare missions require the craft involved to be able to operate for long periods of time – a multi-rotor UAV is unsuitable for this task without landing. Agricultural perch-and-stare missions would greatly benefit from the ability to land on a vantage point.

Fig 1: Typical agricultural fence with strainer post in center

While perching for UAV systems in general has been explored by other researchers, no literature exists specifically for perching of UAVs on any form of upright post or cylinders, with most perching solutions focusing on horizontal branches. Three main classes of existing mechanisms in literature have been identified: biologically inspired, surface adhesion with end effectors and hook-based solutions.

Biologically inspired designs are mainly derivatives of anisodactyl or zygodactyl bird claws and flexure tendons gripping around a horizontal post. Lee *et al* [3] and Doyle *et al* [4] have both investigated passive four-bar linkage based mechanisms for this purpose with success under static loading scenarios, but neither team attempted landing tests. Erbil et al. [5] have also designed a similar mechanism with interlocking digits and a screw-drive mechanism for actuation.

Another identified method for perching on surfaces is the use of end effectors which directly interact with the relevant surface. Desbiens and Cutkosky [6] proposed a perching method for fixed-wing UAVs through the usage of microspines, small spikes which physically interfere and dig into a smooth or rough surface to provide a holding force. A team from Stanford University [7] has adapted this concept for their SCAMP robot, combining a multi-rotor and a microspine based perching mechanism on a multi-rotor UAV. Other takes on the use of an end effector also exist, such as Wopereis et al. [8], using a suction cup to perch onto smooth surfaces.

A third method of perching was using hooks. Lee *et al.* [3] implemented a hook style mechanism to perch on the bottom of horizontal surfaces, a soft strip of material prevents the UAV from slipping out once perched. US Patent US20170023948 [9] follows this approach with hooks on fixed-wing UAVs to both perch and dissipate excess kinetic energy.

Autonomous flight is also relevant, with the intent of reducing the training requirements for the operator. While object tracking and automated landing has been researched by other teams in the past, no team has attempted to land on a non-flat surface. Lange *et al.* [10] have demonstrated a precision landing system based on OpenCV and circularity detection of a feature rich landing pad in real-time with an embedded computer; control of the craft is achieved using an optical flow sensor and a sonar. An alternative take on this was completed by Yang *et al.* [11] using artificial neural nets for landing target classification. Wenzel *et al.* [12] and the IR Lock team [13] both implemented an IR beacon based tracking method for automated landing using a Wii Remote camera and a modified CMUCam5 Pixy camera respectively, with the IR Lock code being publicly accessible and implemented as part of the Open Source ArduCopter Project.

T. Lin (tlin442@aucklanduni.ac.nz), S. Long (slon595@aucklanduni.ac.nz) and K. A. Stol (k.stol@auckland.ac.nz) are with the Department of Mechanical Engineering, The University of Auckland, Auckland, New Zealand

This paper outlines the development and performance evaluation of two mechanisms for perching atop standard agricultural full-round timber posts. Methods of automating this process have also been explored, with an emphasis placed on using readily accessible methods.

II. Perching Mechanisms

In New Zealand, there are three size classifications of agricultural full round strainer posts, the sizes being the #1 (200mm+), #2 (175-199mm) and #3 (150-174mm). Hence, any mechanism designed will need to conform to this range of sizes. For simplicity our design target was the #2 strainer post with a diameter of approx. 175mm. The main requirements for mechanism designs are summarized below:

- Can perch on top of standard full round strainer posts with diameter 150-200mm.
- Can perch around any fencing wire attached.
- Allows for a mechanism-to-post misalignment of 25%, approx. 5cm with a #2 strainer.
- Does not damage itself or the post when perching.

To generate concepts, different gripper joint arrangements and actuation methods were explored. Combining them and performing a cost-benefit analysis resulted in two main classes of mechanisms. These being a revolute and a linear prismatic arrangement. The revolute arrangement, consisting of digits spaced out around a central axis, shown in Fig 2(a) and the linear prismatic, with digits actuating linearly, shown in Fig 2(b).

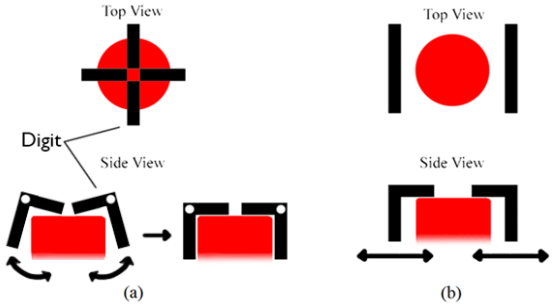

Fig 2: Simplified top and side views for a revolute arrangement (a) and linear prismatic arrangement (b). Approximate post profile shown in red

A. Passive Revolute Mechanism

The overall mechanism consists of four digits in a plus pattern, with each allowed to actuate independently to align the multirotor UAV with the top of the post. In contrast to the original concept, each of the digits instead consists of a parallel four bar linkage, where the radial arrangement allows the digits to conform to the shape of the top of the post. This creates a four degree-of-freedom mechanism which couples into a single degree-of-freedom mechanism with perfect alignment to the post. The final mechanism weighed 347g, allowing for a total of 50mm misalignment from the center of a 175mm post. A servo motor driven locking mechanism was attached to the end of each support arm, but due to time constraints the electrical and control aspects were not implemented. The closed and open position are shown in Fig. 3 (a) and (b) respectively.

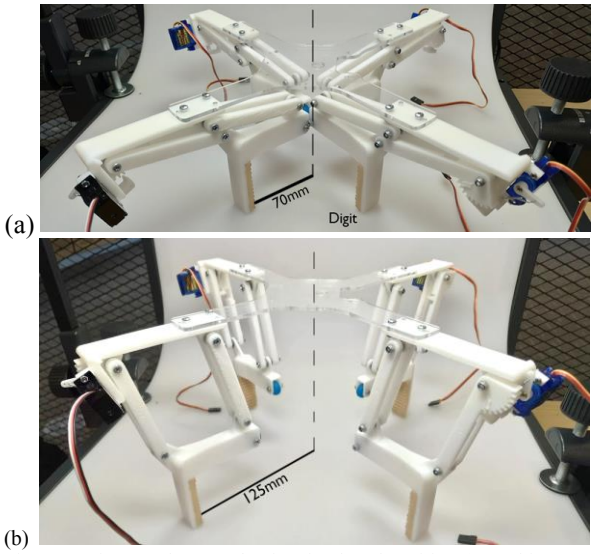

Fig 3: Passive revolute mechanism in closed position (a) and in open position (b)

B. Linear Prismatic Mechanism

The active, motor driven mechanism relies on an electric motor actuating a single degree-of-freedom prismatic joint. This is achieved by coupling the motor shaft to a threaded rod which acts as a screw drive, moving a pair of digits along two slide rails to towards an opposing fixed pair seen in Fig 4. An Arduino and motor shield is used to control the motor and a limit switch is used as a sensor. The stall current of the motor is used to detect when the mechanism has fully actuated. The mechanism weighs 450g and an allowed misalignment of -20 to 70mm in the x and ±20mm in the y direction.

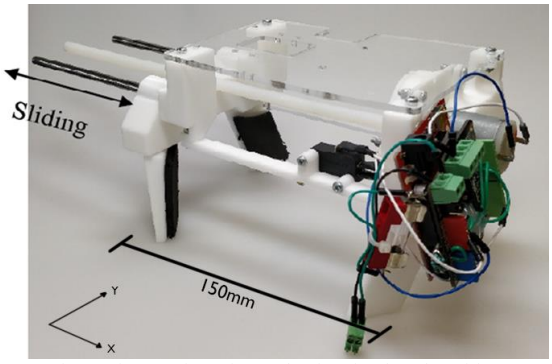

Fig 4: Linear prismatic mechanism in closed position

C. Effects on power and energy

A study by Baluta *et al.* [14] suggested a simplified model for power usage of a propeller when generating a certain amount of thrust. Given the mass of an unmodified craft being 1200g, the addition of a 450g mechanism as payload would result in an approximately 61% increase in energy requirements, while adding a 450g battery pack would approximately double the energy capacity of the craft. Due to this, carrying the mechanism would approximately halve the hover time of the UAV compared to a battery of equivalent mass. Constructing the mechanisms with lighter materials such as carbon fiber would partially mitigate this.

III. Static Testing

When the UAV is in a perched state, the only significant load to be exerted on it is from wind loading. For simplicity, the nominal wind force was assumed to be equal to the required horizontal thrust for a 1.8kg craft tilted by 20°, equating to 6.4N. To ensure we acquire adequate test data we have loaded each mechanism up to approximately 8N of force in the lateral direction and compared the two mechanisms to a weighted acrylic plate as control, simulating the multirotor UAV on top without any mechanism attached.

A test jig was constructed (Fig. 5), consisting of a fixture and the end section of a standard #2 strainer. Each mechanism is set up with a 1.25kg weight on top to simulate the weight of the multirotor UAV. Nylon cable is then used to translate a gravitational load by fixing one end to the mechanism and the other end to a suspended weight. Testing was completed by positioning the mechanism in a perched position, attaching the weight and gradually adding more weight until the mechanism dislodged itself from the top of the post.

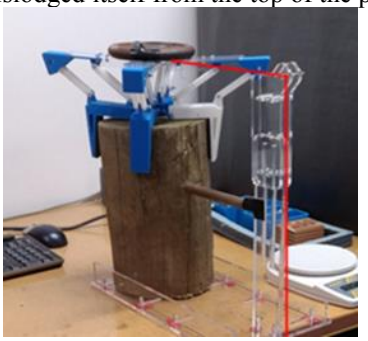

Fig 5: Test jig used with load line shown in red

Five types of loading scenarios were simulated in separate tests. Two extremes of loading configurations were tested for each mechanism, where the loading force is transmitted either normal to the digits' contact surface or at the maximum angle away from the normal direction as shown in Fig 6. A total of eight trials were conducted for each of the loading scenarios

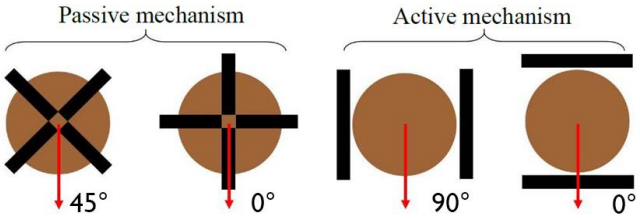

Fig 6: Loading scenarios tested for each mechanism

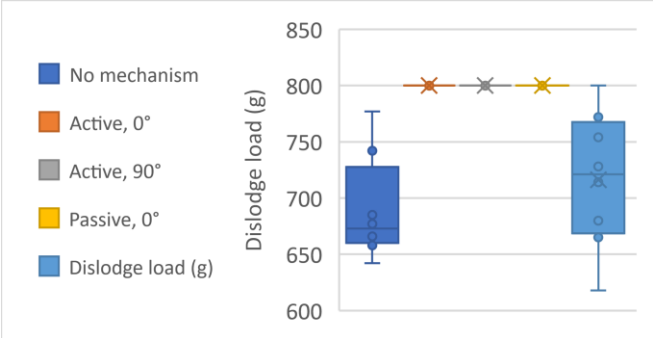

Fig 7: Results of static load testing

After testing the five loading scenarios, it was found that the active mechanism was more resilient to lateral loads, reaching the 800g threshold with every test conducted. The passive mechanism showed similar performance when receiving the load directly through the digit, however was not as effective when loaded between two digits. In this configuration, the mechanism still has a similar range to the control (135g and 182g, with means of 689g and 716g) but with the range of the control fully encapsulated in its range, it cannot be said that it is more resilient to loading for this configuration. It is suspected the reason for failure on reaching our limit of 800g on the remaining off-axis load case on the passive mechanism was mostly due to flexure and deformation of the linkage and associated mounting fixture. This would likely be remedied by switching to a stiffer material such as aluminum or carbon fiber.

To verify the maximum permissible horizontal displacement in the x and y directions relative to the center of mass of the craft for each mechanism, we attached a marker pen to the center of each mechanism and dropped it from a height of 5mm onto the top of a standard #2 strainer post with an indicator on top. Tests were conducted by successively dropping the mechanism at increasing distances from the center in the x and y directions with a successful test being one where the mechanism successfully engages. These distances of successful perches from the center were then measured; the permissible landing region for each mechanism is shown in Fig 8.

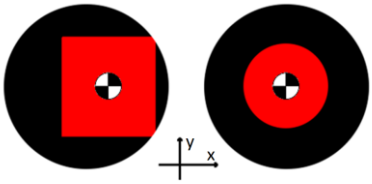

(a) (b)

Fig 8: Permissible landing regions of (a) linear prismatic mechanism and (b) passive revolute mechanism. CoM of multirotor UAV marked

The passive mechanism could successfully actuate and perch provided the center of the mechanism is within 50mm of the center of the post. The linear prismatic mechanism could successfully perch with a x distance of -20 to +70mm and a y distance of ±60mm relative to the centre of the post. Note the ideal landing position for the linear prismatic mechanism is skewed towards one side, this was by design to avoid offsetting the centre of mass of the UAV during flight.

IV. Autonomous Landing Method

A modified version of ArduCopter's Precision Landing [15] functionality with GPS requirements removed. As part of this, the CMUCam5 Pixy vision sensor was used to track the top of the post and a MaxBotix XL-EZ4 sonar sensor was used to track the altitude of the craft. Precision Landing uses the pixel position of the target in the Pixy's frame and the current altitude read from the sonar to estimate the x and y distance of the UAV to the target. The internal waypoint controller is then used to navigate the UAV to the correct location while the altitude is steadily decreased.

As the CMUCam5 Pixy relies on color detection for rapid blob tracking, it is very important that the chosen color present on the blob is distinctly different from every other color to avoid incorrect detection of landing targets. Using a custom OpenCV program and photos taken of standard agricultural posts the HSV values are extracted using:

$$H_i = \sum_{j=1}^{j=ncol} \sum_{k=1}^{k=nrow} \frac{Hue(j,k)}{n} \quad (1)$$

$$Hue(j,k) = \begin{cases} 1 \; if \; Hue \; at \; (j,k) = i \\ 0 \; otherwise \end{cases} \quad (2)$$

Where H_i is the normalized value of hue angle i° and n is the total number of pixels in the image. j and k are pixel locations within the source image in Fig. 9(a). Using three images around a typical agricultural post, a histogram was generated by summing the results in Fig. 10 below.

(a) (b)

Fig. 9: (a) Sample image used for hue discrimination (b) image of marker to be placed on top of post

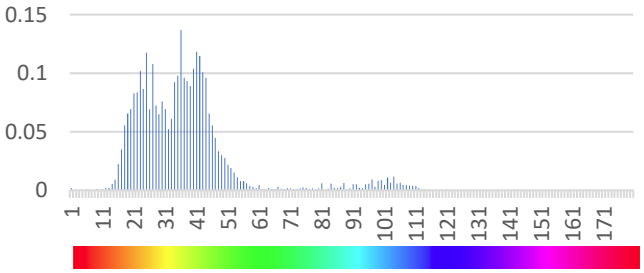

Fig. 10: Histogram of hue values for images taken around an agricultural fence post.

From this, we can see that there is a lack of pixels with a hue value ranging between 115°-179° as well as between 62° to 85°. The middle of these ranges corresponds to the colour of magenta and cyan respectively, making these colours a suitable pick for our target. To avoid other hue values which may be present in the scene, we have chosen to use a magenta coloured target as shown in Fig. 9(b). Due to the limited number of images analyzed, there may be scenarios where false positives arise. These would be revealed during field testing and could subsequently be corrected by changing the hue of the target.

V. Flight Testing

A. Precision Landing Characterization

The purpose of this experiment is to quantify the accuracy of the automated landing system. Additionally, this data is used with data from the misalignment experiment to find an expected success rate of the mechanisms using previous misalignment data. To characterize the landing performance of ArduCopter's Precision Landing system, all mechanisms were removed from the UAV and the craft was flown up to approximately shoulder height and set to precision land mode with the target atop an approx. 40cm section of a standard #2 strainer post. A Vicon motion capture system was used to capture the absolute position of both the UAV and the post. The first capture was conducted as a calibration capture, with the UAV being placed in the expected perfect landing position on top of the post. 30 trials were conducted and the final landing position is recorded:

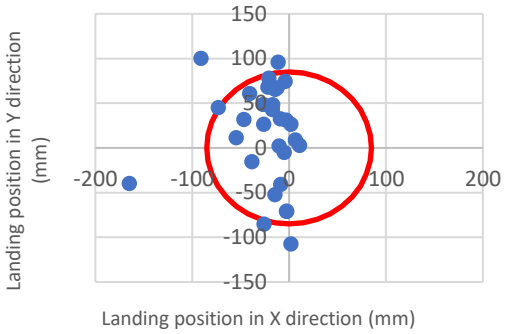

Fig 11. Final landing positions. Post profile shown in red

The mean offset distance was found as 61mm, with a standard deviation of 37mm. As shown from the scatter plot in Fig 11 of landing positions, the precision landing results do seem to have an offset towards the negative X-direction. We suspect this was due to imperfect alignment of the camera and was remedied for later tests. Normality of the data was tested using Normal Q-Q plots, where the data appeared to be scattered about a straight line, with a R^2 value of 0.59 and 0.82 for the x and y directions respectively.

Assuming the perching success of each mechanism is primarily dependent on the accuracy of which Precision Landing can maneuver the UAV to the center of the post, we determined the theoretical probability of a successful perch. This is completed by assuming a standard normal distribution with mean and standard deviation from the characterization test (Fig. 11). The probability in which a landing would fall within the permissible region from the experimental landing offset test was determined and summarized in Table I. below.

TABLE I. THEORETICAL SUCCESS RATES

Pole Size	Passive Revolute	Active Prismatic
150mm	73%	80%
175mm	62%	71%
200mm	49%	60%

B. Dynamic Performance of Mechanism

To validate our claim where the landing performance of each mechanism is largely dependent on the landing accuracy, flight tests were conducted. The UAV was flown to approximately shoulder height with each mechanism attached, then set to automatically land and perch on top of a small section of the three common strainer post sizes with diameters 150mm, 175mm and 200mm. The UAV is left undisturbed after each perch to determine the success or failure of the perch, with a successful perch being defined as

one where the UAV rests on top of the post in a stable position. A control sample with a flat acrylic disc with diameter 130mm attached was used as a basis of comparison. Each mechanism was tested 15 times on each post size to determine success rate and durability. While the methodology employed inevitably couples the performance of the UAV landing controller with that of the mechanism, the intent is to verify our assumption where perching success rate is mainly dependent on landing accuracy of the controller.

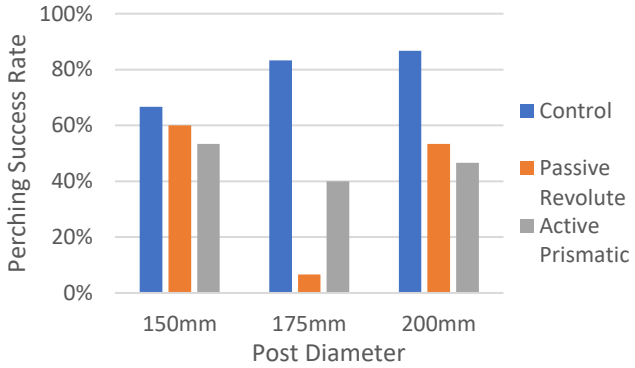

Fig 12: Landing success rate by post size

With the current configurations both mechanisms consistently performed worse than our control test with success rates being between 7% worse at the best case and 77% worse at the worst case. Landing success rate as expected increases as the size of the post is increased for the control as the allowed landing area increases. Both mechanisms followed a trend completely opposite of the control, with performance on the larger post sizes being worse than that on the smaller size. There is relatively little performance difference between the two mechanisms at a post diameter of 150mm, with the passive mechanism performing 7% worse than the control. As this essentially amounts to a single additional landing for the control, this difference is well within the margin of error with our number of samples, suggesting the performance of the passive mechanism is quite similar compared to having no mechanism for the 150mm diameter post. One element which contributed to this increased percentage of successful trials identified was that with the smallest 150mm post, the mechanism would partially engage, with only two or three of the digits collapsing on landing. This effect appeared to allow the passive mechanism to obtain a stable perch even without all digits being actuated. Further development based on this concept could potentially improve the performance of the mechanism for other post sizes.

Fig 13: Partial engagement of passive mechanism on 150mm post

The results varied wildly for the 175mm sized pole, with the passive mechanism performing 77% worse than the control. Observations during testing suggested that failure with this post size is likely attributed to the mechanisms inability to cancel out horizontal velocities after the perch, causing the UAV to dislodge itself after landing. Results for the larger 200mm post is as expected.

The Active Prismatic mechanism appears to be performing badly on the 150mm diameter post, however of the 7 failed runs during our testing, 5 of them was due to the screw drive not triggering as the limit switch did not contact the top of the post; assuming the limit switch was triggered correctly, this would result in an 87% success rate for a post with diameter 150mm.

TABLE II. COMPARISON OF THEORETICAL AND EXPERIMENTAL SUCCESS RATES

Passive Revolute Success Rate			
Post Size	Theoretical	Actual	Difference
150mm	73%	60%	**-13%**
175mm	62%	7%	**-55%**
200mm	49%	53%	**+4%**
Active Prismatic Success Rate			
Post Size	Theoretical	Actual	Difference
150mm	80%	87%	**+7%**
175mm	71%	40%	**-31%**
200mm	60%	47%	**-13%**

Comparing the theoretical and actual success rates we can see that with exception of the 175mm diameter post, both mechanisms performed relatively similarly to their theoretical performance values, with every difference being within ±13%. This validates our assumption for the 150mm and 200mm sized post, where the dynamic landing performance of each mechanism appears to be mostly dependent on the accuracy of the landing.

C. *Influence of Wind*

The final series of tests accessed landing success rate with regards to the effect of wind. Two large fans were used that applied a wind speed of approximately 4m/s to the UAV's descent path. All trials were conducted with the UAV flown to approximately shoulder height and set to automatically land. 10 trails were completed for each mechanism on a post with diameter 175mm, with the results shown in Fig. 14 below.

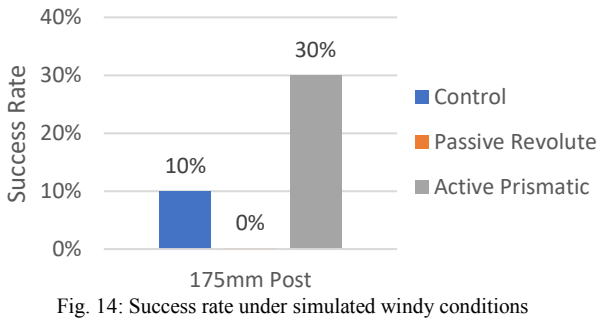

Fig. 14: Success rate under simulated windy conditions

The success rate of our control experiment reduced from 83% to 10%. In comparison, the passive revolute mechanism appears to have severe difficulty accounting for wind loading, failing all 10 attempts. In contrast, the active prismatic mechanism succeeded in 3 of 10 attempts, demonstrating superior ability in perching under wind conditions. The landing performance of Precision Landing was not tested rigorously under windy conditions. However, observations during preliminary tests show most failed landings were due to landing accuracy and not mechanism actuation.

As a final test, the UAV and the associated active prismatic mechanism was flown outdoors. The magenta target was set up on a single post on a farm fence and landing was attempted multiple times; none were successful. ArduCopter's Precision Landing was unable to land sufficiently accurately to perch on top of the post. It is suspected that this could be due to excessive wind during testing, non-ideal controller tuning or incorrect altitude estimation. Further work will need to be done to verify shortcomings of the controller. The final actions of the craft before evasive maneuvers is in Fig. 15.

Fig. 15: UAV attempted landing

VI. Conclusions

This paper presents initial work on autonomous landing of multi-rotor UAVs atop fence posts in an agricultural setting. Two mechanisms were designed to handle this, a passive weight actuated design and an active prismatic design. Results indicate that the passive weight actuated mechanism with an added lock performed consistently better compared to having no mechanism for on-axis loads. However, rigidity issues still affect its ability to withstand off-axis loads. The active linear prismatic mechanism consistently performed better compared to having no mechanism in both on-axis and off-axis directions.

Investigations into the colors present near a standard agricultural fence post suggest a magenta colored target is most suitable. Characterization of ArduCopter's Precision Landing showed it is capable of landing on top of a target with a mean radial absolute position error of 61mm with a standard deviation of 37mm. This relationship appears to be normally distributed.

Flight testing suggests that dynamic performance of both mechanisms increase with decreasing post size, which is contrary to the control where performance increases with increasing post size. Both mechanisms perform worse than having no mechanism during windless conditions for post diameter 175mm and larger. Performance for 150mm diameter posts is on par or better compared to no mechanism. Dynamic tests with wind suggest the active prismatic mechanism performs better than having no mechanism in conditions where wind forces are present. The passive mechanism appears to have its performance decreased further in the presence of wind with a lower success rate compared to no mechanism.

Further work could be completed on the controller and visual tracking aspects, as it was found that ArduCopter's Precision Landing was inadequate when dealing with wind disturbances and non-flat landing surfaces. Alternative vision systems could be investigated to provide a more accurate and robust position estimate of the target.

References

[1] Jiang, S., Jiang, W., Huang, W., & Yang, L. (2017). UAV-Based Oblique Photogrammetry for Outdoor Data Acquisition and Offsite Visual Inspection of Transmission Line. Remote Sensing, 9(3), 278. doi:10.3390/rs9030278

[2] Candiago, S., Remondino, F., Giglio, M. D., Dubbini, M., & Gattelli, M. (2015). Evaluating Multispectral Images and Vegetation Indices for Precision Farming Applications from UAV Images. Remote Sensing, 7(4), 4026-4047. doi:10.3390/rs70404026/

[3] Lee, C. (2014). Passive Systems and Underaction in Our Perching Landing Gear. Retrieved April 24, 2017, from http://faculty.olin.edu/~clee1/plg.html

[4] Doyle, C. E., Bird, J. J., Isom, T. A., Kallman, J. C., Bariess, D. F., Dunlop, D. J., Minor, M. A. (2013, April). An Avian-Inspired Passive Mechanism for Quadrotor Perching. IEEE/ASME Transactions on Mechatronics, 18(2), 506-517. doi:10.1109/TMECH.2012.2211081

[5] Erbil, M., Prior, S., & Keane, A. (2013). Design Optimisation of a Reconfigurable Perching Element for Vertical Take-Off and Landing Unmanned Aerial Vehicles. International Journal of Micro Air Vehicles, 5(3), 207-228. doi:10.1260/1756-8293.5.3.207

[6] Desbiens, A. L., & Cutkosky, M. R. (2009). Landing and Perching on Vertical Surfaces with Microspines for Small Unmanned Air Vehicles. Selected papers from the 2nd International Symposium on UAVs, Reno, Nevada, U.S.A. June 8–10, 2009, 313-327. doi:10.1007/978-90-481-8764-5_16

[7] Pope, M. T. Retrieved April 25, 2017, MultiModalRobots from http://bdml.stanford.edu/Main/MultiModalRobots#SCAMP

[8] Wopereis, H. W., Molen, T. D., Post, T. H., Stramigioli, S., & Fumagalli, M. (2016). Mechanism for perching on smooth surfaces using aerial impacts. 2016 IEEE International Symposium on Safety, Security, and Rescue Robotics (SSRR). doi:10.1109/ssrr.2016.7784292

[9] Peverill, J., & Mckenna, T. (2017). U.S. Patent No. US20170023948. Washington, DC: U.S. Patent and Trademark Office.

[10] Lange, S., Sunderhauf, N., Protzel, P., A vision based onboard approach for landing and position control of an autonomous multirotor UAV in GPS-denied environments, Proc. of Conf. on Advanced Robotics, pp. 1-6, Munich, June 2009

[11] Yang, S., Scherer, S. A., & Zell, A. (2012). An Onboard Monocular Vision System for Autonomous Takeoff, Hovering and Landing of a Micro Aerial Vehicle. Journal of Intelligent & Robotic Systems, 69(1-4), 499-515. doi:10.1007/s10846-012-9749-7

[12] Wenzel, K. E., Masselli, A., & Zell, A. (2010). Automatic Take Off, Tracking and Landing of a Miniature UAV on a Moving Carrier Vehicle. Journal of Intelligent & Robotic Systems, 61(1-4), 221-238. doi:10.1007/s10846-010-9473-0

[13] Infrared Tracking Systems for Drones and Robot Automation. (n.d.). Retrieved April 26, 2017, from https://irlock.com/

[14] Baluta, S. (2015). How much power is needed to hover ? Retrieved from http://www.starlino.com/power2thrust.html

[15] Precision Landing and Loiter with IR-LOCK. Retrieved February 13, 2018, from http://ardupilot.org/copter/docs/precision-landing-with-irlock.html